JACS
JOURNAL OF THE AMERICAN CHEMICAL SOCIETY
Article
pubs.acs.org/JACS

Mammalian Frataxin Controls Sulfur Production and Iron Entry during de Novo Fe_4S_4 Cluster Assembly

Florent Colin,[†,‡,§,∥,⊥] Alain Martelli,[†,‡,§,∥,⊥] Martin Clémancey,[#] Jean-Marc Latour,[#] Serge Gambarelli,[▽] Laura Zeppieri,[†,‡,§,∥,⊥] Catherine Birck,[‡,§,∥,○] Adeline Page,[†,‡,§,∥] Hélène Puccio,*[,†,‡,§,∥,⊥] and Sandrine Ollagnier de Choudens*[,◆]

[†]Translational Medicine and Neurogenetics, Institut de Génétique et de Biologie Moléculaire et Cellulaire (IGBMC), Illkirch, France
[‡]INSERM, U596, Illkirch, France
[§]CNRS, UMR7104, Illkirch, France
[∥]Université de Strasbourg, Strasbourg, France
[⊥]Collège de France, Chaire de Génétique Humaine, Illkirch, France
[#]DSV/iRTSV/CBM, UMR 5249 CEA-Université Grenoble I-CNRS/Equipe de Physicochimie des Métaux en Biologie, CEA-Grenoble, 17 Rue des Martyrs, 38054 Grenoble Cedex 09, France
[▽]DSM/INaC/SCIB UMR-E3 CEA-UJF/Laboratoire "Laboratoire de Résonance Magnétique", CEA-Grenoble, 17 Rue des Martyrs, 38054 Grenoble Cedex 09, France
[○]Structural Biology and Genomics Platform, Institut de Génétique et de Biologie Moléculaire et Cellulaire (IGBMC), Illkirch, France
[◆]DSV/iRTSV/CBM, UMR 5249 CEA-Université Grenoble I-CNRS/Equipe Biocatalyse, CEA-Grenoble, 17 Rue des Martyrs, 38054 Grenoble Cedex 09, France

Supporting Information

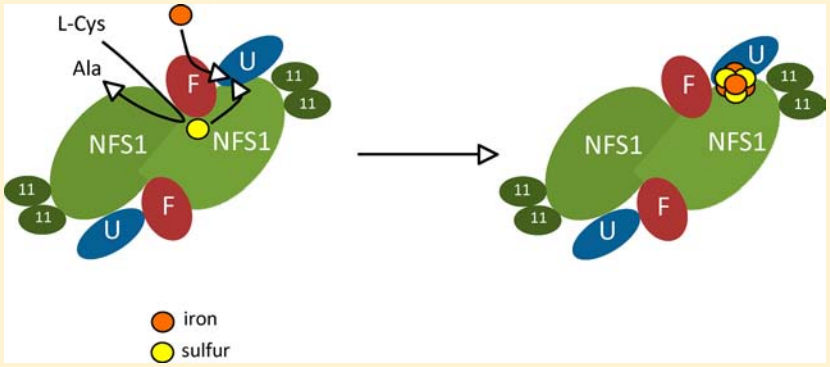

ABSTRACT: Iron−sulfur (Fe−S) cluster-containing proteins are essential components of cells. In eukaryotes, Fe−S clusters are synthesized by the mitochondrial iron−sulfur cluster (ISC) machinery and the cytosolic iron−sulfur assembly (CIA) system. In the mammalian ISC machinery, preassembly of the Fe−S cluster on the scaffold protein (ISCU) involves a cysteine desulfurase complex (NFS1/ISD11) and frataxin (FXN), the protein deficient in Friedreich's ataxia. Here, by comparing the biochemical and spectroscopic properties of quaternary (ISCU/NFS1/ISD11/FXN) and ternary (ISCU/NFS1/ISD11) complexes, we show that FXN stabilizes the quaternary complex and controls iron entry to the complex through activation of cysteine desulfurization. Furthermore, we show for the first time that in the presence of iron and L-cysteine, an $[Fe_4S_4]$ cluster is formed within the quaternary complex that can be transferred to mammalian aconitase (mACO2) to generate an active enzyme. In the absence of FXN, although the ternary complex can assemble an Fe−S cluster, the cluster is inefficiently transferred to ACO2. Taken together, these data help to unravel further the Fe−S cluster assembly process and the molecular basis of Friedreich's ataxia.

INTRODUCTION

Iron−sulfur (Fe−S) clusters are critical redox-active prosthetic groups that are present in proteins involved in numerous essential cellular processes.[1,2] While the predominant functions of Fe−S clusters are in electron transfer and radical generation, they also participate in substrate binding and activation, protein stabilization, and regulation of gene expression or enzyme activity. Within the past decade, the biogenesis of Fe−S proteins has been extensively studied by genetic and biochemical approaches in bacteria and yeast and more recently in plants and mammals, and this work has demonstrated that it

Received: September 3, 2012
Published: December 22, 2012

   dx.doi.org/10.1021/ja308736e | J. Am. Chem. Soc. 2013, 135, 733−740

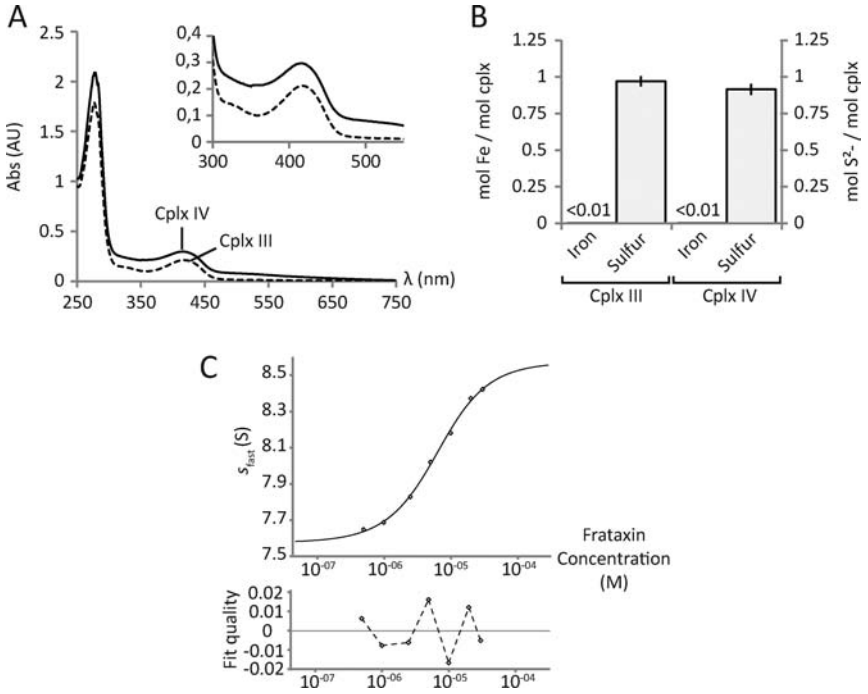

Figure 1. Characterization of ternary and quaternary complexes. (A) UV−vis spectra of as-purified CplxIII (dashed line) and CplxIV (solid line). Inset: focus on the 300−500 nm region of the UV−vis spectra. (B) Iron and sulfur contents of as-purified CplxIII and CplxIV. In the assay, cysteine was converted to alanine, and the resulting persulfide was reduced with dithiothreitol (DTT) and detected as sulfide. (C) Signal-averaged value of the sedimentation coefficient at the reaction boundary (s_{fast}) as a function of loading concentration for each sedimentation coefficient (s) distribution. The best-fit binding isotherm (solid line) was obtained for parameter estimates of K_{d1} = 2.6 μM, K_{d2} = 10.3 μM, s_A = 7.58 S, s_B = 2.06 S, s_{AB} = 8.09 S, and s_{ABB} = 8.58 S using a heteroassociation model involving CplxIII (component A) with two equivalent binding sites for FXN (component B).

is a complex process involving multiple components.[1−3] Most of the components of the general "housekeeping" biosynthetic iron−sulfur cluster (ISC) machinery are highly conserved in almost all organisms, and several human orthologues are implicated in severe disorders,[4] pointing to the importance of this pathway for normal cellular function.

The initial stage of nascent Fe−S cluster biosynthesis, which is accomplished by a multimeric protein complex, involves the assembly of a transiently bound Fe−S cluster on a scaffold protein (IscU in bacteria, Isu1 in yeast, or ISCU in mammals) from inorganic sulfur and iron. The sulfur is provided through a persulfide intermediate by a pyridoxal phosphate (PLP)-dependent cysteine desulfurase (IscS in bacteria, Nfs1/Isd11 in yeast, or NFS1/ISD11 in mammals). Although its exact function is unknown, the eukaryotic protein ISD11 has been proposed to stabilize NFS1 through a direct interaction and to activate the enzyme through a conformational change.[5−7] The scaffold and the cysteine desulfurase interact to form in bacteria an $\alpha_2\beta_2$ heterotetrameric complex, thus promoting direct sulfur transfer.[8−10] The sources of the iron and the required electrons have not been clearly identified, although frataxin and ferredoxin have been suggested as the iron and electron donors, respectively.[11,12] Once assembled, the scaffold-bound Fe−S clusters are transferred to target proteins with the help of accessory proteins and factors.[1,2] In eukaryotes, the assembly of the nascent Fe−S clusters takes place in the mitochondria.

Frataxin is a conserved small globular mitochondrial protein whose reduced expression causes the severe neurodegenerative disease Friedreich's ataxia by impairing Fe−S cluster biogenesis and iron metabolism.[13,14] Although frataxin has been proposed to be a multifunctional protein involved in different iron-dependent mitochondrial pathways, phylogenetic, genetic, and biochemical studies point to the essential role of frataxin in Fe−S metabolism.[15−19]

Early in vitro studies of bacterial, yeast, or human frataxin showed a mild to low affinity for ferrous iron (3−55 μM range) through an interaction with a conserved acidic ridge of the mature protein.[20−22] The proposed function of frataxin as an iron donor was suggested by both the iron-dependent interaction of yeast frataxin with Nfs1 and Isu1[23] and in vitro studies demonstrating the capacity of iron-loaded mature human frataxin to provide iron for Fe−S cluster formation on ISCU.[20] Frataxin has also been shown to form oligomers in the presence of iron in vitro, initially suggesting an iron detoxification and storage function for frataxin.[11,24,25] However, this hypothesis has been questioned in vivo. Indeed, the deletion of yeast frataxin can be complemented by a frataxin mutant defective in iron-induced oligomerization.[26] Furthermore, the mature form of human frataxin (FXN_{81-210}), which has been shown not to oligomerize,[27] rescued the cellular viability of murine fibroblasts deleted for frataxin.[16] Both of these results indicate that the formation of oligomers is not a requisite for frataxin to be functional. On the other hand, in vitro reconstitution experiments showed that oligomeric iron-loaded bacterial (CyaY) and yeast (Yfh1) frataxins could provide iron for Fe−S cluster formation on the scaffold protein (IscU/Isu1).[11,20] More recently, the possibility that frataxin might act as a regulator of cysteine desulfurase activity (positive in eukaryotes or negative in prokaryotes) has emerged.[15,17]

Using a coexpression approach, we previously showed that murine frataxin interacts in an iron-independent manner with a preformed ternary complex composed of NFS1, ISD11, and ISCU, thus leading to a quaternary complex.[16] To dissect further the role of frataxin in the first step of Fe−S biogenesis in

dx.doi.org/10.1021/ja308736e | J. Am. Chem. Soc. 2013, 135, 733−740

mammalian eukaryotes, we studied and compared the biochemical and biophysical properties of the recombinant ternary (CplxIII) and quaternary (CplxIV) complexes in the presence of the two key substrates of Fe−S assembly, iron and cysteine. Herein we report for the first time that mammalian frataxin controls iron entry on CplxIV through activation of its cysteine desulfurase activity, allowing the formation of $[Fe_4S_4]$ clusters.

RESULTS AND DISCUSSION

Structural and Enzymatic Characterization of Ternary and Quaternary Complexes Formed in Vivo in a Heterologous System. To determine the role of frataxin in the early steps of Fe−S formation, as a prerequisite, we biochemically and functionally characterized the as-purified recombinant CplxIII and CplxIV complexes formed in vivo (see the Supporting Information). Pure CplxIII has a mass of 161 052 Da as determined by electrospray ionization time of flight (ESI-TOF) mass spectrometry, in agreement with the mass of 160 kDa estimated from the retention time on gel filtration (Figure S1 in the Supporting Information). This suggests a homodimeric complex in which each unit has a 1:2:1 NFS1:ISD11:ISCU stoichiometry. CplxIV eluted as a single peak with an apparent molecular weight of 185 kDa (Figure S1 in the Supporting Information), in agreement with the reported mass of 189 623 Da,[16] also suggesting a homodimeric organization in which each unit has a 1:2:1:1 NFS1:ISD11:ISCU:FXN stoichiometry. As-purified CplxIII and CplxIV displayed a yellow color (absorption band at 420 nm) corresponding to PLP bound on NFS1 (1.9 and 1.7 ± 0.1 PLP/Cplx, respectively) (Figure 1A) but were devoid of iron (<0.01 Fe/Cplx) and contained small amounts of sulfur (0.97 ± 0.04 S/CplxIII and 0.91 ± 0.05 S/CplxIV), likely in a persulfide intermediate form on NFS1 (Figure 1B). In contrast to CplxIII, which precipitated upon freezing−thawing, CplxIV was stable toward freezing−thawing, suggesting a stabilizing effect of frataxin for CplxIII. Interestingly, a quaternary complex (named the "quaternized complex") can be formed from pure CplxIII and free monomeric frataxin (Figure S1 in the Supporting Information). To determine the affinity of frataxin for CplxIII, we performed analytical ultracentrifugation (AUC) sedimentation velocity experiments using different CplxIII:FXN ratios (Figure 1C; see the Supporting Information for details). In the titration of CplxIII with increasing concentrations of FXN, the peak in the sedimentation complex [*s*, measured in svedbergs (1 S = 10^{-13} s)] for the complex exhibited a concentration-dependent movement characteristic of a rapidly interacting system (Figure 1C). The peak for CplxIII alone (7.45 S) was shifted toward the *s* value of 8.6 S expected for a 1:2 CplxIII:FXN complex through an intermediate *s* value of 8.1 S expected for a 1:1 CplxIII:FXN complex. Data analysis of the signal-averaged *s* value at the reaction boundary (s_{fast}) as a function of loading concentration gave estimated K_d values of ~2.6 μM (K_{d1}) and 10.3 μM (K_{d2}) for the 1:1 and 1:2 complexes, respectively.

Both CplxIII and CplxIV were endowed with cysteine desulfurase activity carried by the NFS1 protein, which we evaluated by measuring alanine and sulfide production (Figure S2A in the Supporting Information). As-purified CplxIV exhibited Michaelis−Menten kinetics for sulfide production with a Michaelis constant (K_M) of 6.7 μM for cysteine and a k_{cat} of 3.9 min^{-1} (Table 1). The value of k_{cat} decreased by a factor of 5 (k_{cat}= 0.85 min^{-1}) and the K_M increased by a factor of 1.5 (K_M= 10.7 μM) with CplxIII, demonstrating that both k_{cat} and K_M were altered by the presence of FXN (Table 1). The cysteine desulfurase activity was stable over time (2−14 days) for CplxIV, whereas it was dramatically affected for CplxIII after 8 days, indicating a stabilizing effect of frataxin on the enzymatic activity of CplxIII (Figure S2 in the Supporting Information). The quaternized complex displayed a cysteine desulfurase activity similar to that of the as-purified CplxIV (k_{cat} = 3.6 min^{-1}) (Figure 2A), demonstrating that it is the presence of frataxin that enhances the cysteine desulfurase activity. As ferrous iron was reported specifically to enhance by an additional factor of 2 the cysteine desulfurase activity of NFS1/ISD11 in the presence of FXN and ISCU,[15] we explored the sulfide production by both complexes in the presence of iron. Under our conditions, iron ions (Fe^{2+} and Fe^{3+}) had a small stimulatory effect (1.5-fold) on the sulfide production of both CplxIII and the quaternized complex (Figure 2B), but this effect was not specific to iron, since Mn^{2+} and Mg^{2+} gave a similar stimulation. Zn^{2+} had no effect.

Table 1. Kinetic Data for CplxIII and CplxIV Enzymatic Activity

	k_{cat} (min^{-1})	K_M (μM)
CplxIII	0.85	10.7
CplxIV	3.9	6.7

These results provide for the first time a consolidated characterization of mammalian CplxIII and CplxIV. The high level of expression of the complexes as well as the purification steps performed under aerobiosis lead to the isolation of cluster-free complexes. The isolation of both complexes from *Escherichia coli* extracts strongly suggests that they represent functional states for Fe−S cluster biosynthesis and that they are mechanistically relevant species for unraveling the Fe−S biogenesis process. Two observations can be drawn from the stoichiometries of the two complexes. (i) There is conservation with prokaryotes in the organization of the complexes: in the absence of frataxin, there are two cysteine desulfurases and two scaffolds,[9,10] and when frataxin is present, there are two cysteine desulfurases, two scaffolds, and two frataxins.[28] (ii) Mammalian FXN exists within CplxIV as a monomer (per unit of complex) rather than as an oligomeric form, reinforcing in vivo data demonstrating that the essential form is the monomeric one.[16] The AUC experiments confirmed the stoichiometry of two FXN per CplxIV. We also observed that FXN enhances the cysteine desulfurase activity as reported previously,[15] but the kinetic parameters were slightly different, probably reflecting differences in stability and/or homogeneity for as-purified complexes in comparison with complexes obtained by combining purified recombinant proteins. As the physiological concentration of cysteine in eukaryotic cells is 0.1 mM,[29] our data together indicate that FXN greatly stimulates the cysteine desulfurase activity at physiological cysteine concentrations. In addition, our data demonstrate that cysteine desulfurase activation by FXN is iron-independent, in contrast to published results,[15] and that frataxin accounts for the main stimulatory effect of cysteine desulfurase activity. FXN binding and stimulation of the cysteine desulfurase activity are reminiscent of the behavior of sulfur-acceptor proteins in bacterial systems. Indeed, in *E. coli*, the IscS activity is stimulated 6-fold by IscU binding[30] and the SufS activity is increased 50-fold by SufE interactions.[31] Because there is no evidence that FXN directly participates in cysteine desulfurase catalysis and since FXN

dx.doi.org/10.1021/ja308736e | J. Am. Chem. Soc. 2013, 135, 733−740

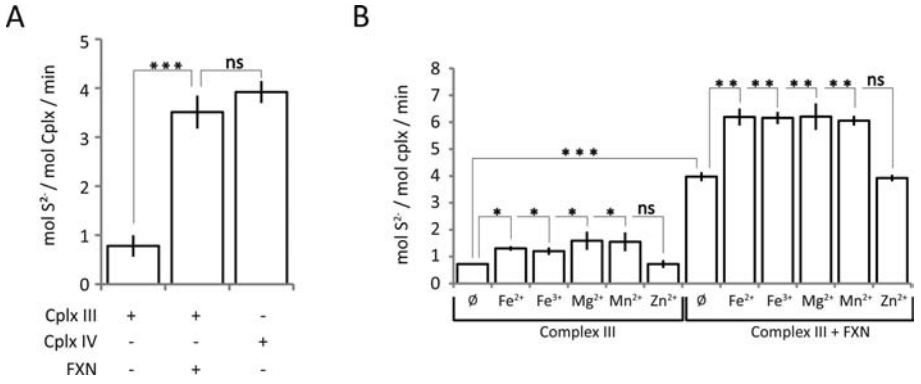

Figure 2. FXN enhances the cysteine desulfurase activity of CplxIII. (A) Cysteine desulfurase activities of CplxIII, CplxIV, and the quaternized complex measured by sulfur quantitation. (B) Effect of a 10-fold molar excess of Fe^{2+} [from $(NH_4)_2Fe(SO_4)_2{\cdot}6H_2O$], Fe^{3+} (from $FeCl_3$), Mn^{2+} (from $MnSO_4$), Mg^{2+} (from $MgCl_2$), or Zn^{2+} (from $ZnSO_4$) on the cysteine desulfurase activity of CplxIII and the quaternized complex. Symbols: ns, nonsignificant; *, $p < 0.01$; **, $p < 0.05$; ***, $p < 0.001$.

stimulates cysteine desulfurization in a ISCU-dependent manner,[15] FXN binding to CplxIII likely induces a conformational change that positions the NFS1 persulfide loop close to a conserved cysteine on ISCU for optimal sulfur transfer, thereby increasing cysteine turnover. Interestingly, the bacterial homologue CyaY displayed an inhibitory effect on Fe–S cluster biogenesis in reconstitution experiments in vitro and was found to decrease the enzymatic activity of IscS in the presence of IscU.[17] However, this difference between the mammalian and bacterial systems appears to be determined by the intrinsic properties of the cysteine desulfurase.[32]

Frataxin Controls Iron Entry in the Quaternary Complex. To investigate whether the presence of frataxin in CplxIV would modulate iron fixation, we compared the iron binding capacities of CplxIII and CplxIV (Figure 3A). The CplxIII Fe^{2+} binding curve suggested a specific ferrous iron fixation that quickly saturated around 1.5 ± 0.12 Fe/Cplx (Figure 3A). On the contrary, CplxIV bound much less ferrous iron, despite a 10-fold molar excess (0.29 ± 0.39 Fe/Cplx). CplxIV did not show better affinity for the ferric form of iron, whereas CplxIII showed a great ability to bind ferric iron (Figure S3 in the Supporting Information). When FXN was added to CplxIII prior to iron, 0.33 ± 0.10 Fe/Cplx was detected, indicating that the quaternized complex had ferrous iron binding properties similar to those of CplxIV (Figure 3B). However, when the iron was added to CplxIII before FXN, 1.1 ± 0.15 Fe/Cplx was detected, a value comparable to that of CplxIII without FXN (Figure 3B). Taken together, these data indicate that frataxin inhibits binding of ferrous and ferric iron to the quaternary complex, which was quite surprising because bacterial and yeast frataxins have clearly been shown to bind and provide iron for Fe–S formation.[11,20] We therefore investigated iron binding to monomeric FXN by incubating FXN with an excess of either ferrous or ferric iron under the conditions used for CyaY.[11] We observed that the mature monomeric form of frataxin could bind ~1 Fe/FXN under all conditions used (Figure S4 in the Supporting Information), showing that FXN has different iron binding behavior when free and complexed. We then investigated whether the cysteine desulfurase activity of the complexes could influence iron entry. While activation of the cysteine desulfurase of CplxIII had no effect on iron binding (Figure 3C), interestingly, the iron content in CplxIV was significantly enhanced upon activation of the cysteine desulfurase. Indeed, roughly 3.5 ± 0.1 Fe/CplxIV were detected, corresponding to a 10-fold increase relative to

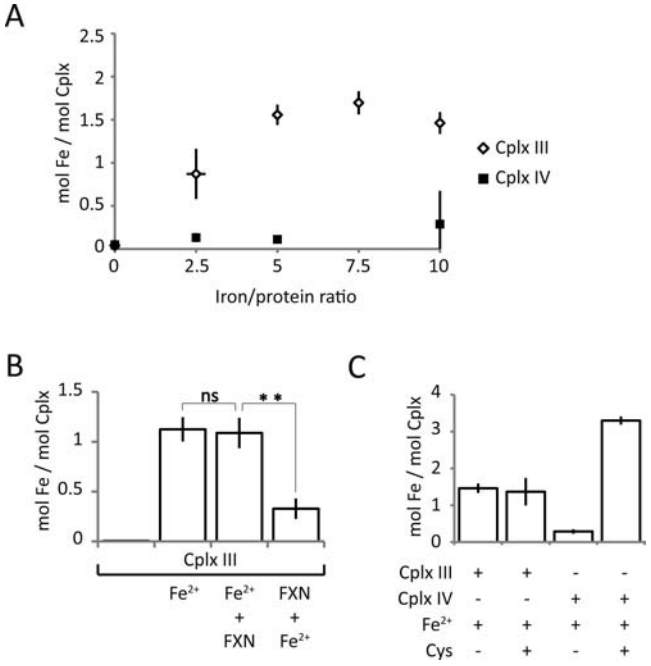

Figure 3. Control of iron entry by frataxin. (A) Iron contents of CplxIII and CplxIV after incubation for 1 h with different molar excess of Fe^{2+} [from $(NH_4)_2Fe(SO_4)_2{\cdot}6H_2O$] and desalting. (B) Iron content of the quaternized complex after incubation with Fe^{2+} added either before or after FXN. (C) Iron content upon activation of the ternary and quaternary complexes' cysteine desulfurase activities (10 equiv of Fe^{2+}, 10 equiv of cysteine, and 50 equiv of DTT followed by desalting). All of the experiments were done under anaerobic conditions. ns, nonsignificant; **, $p < 0.05$.

the amount measured in the absence of cysteine desulfurization (Figure 3C). This increase in iron binding is due to activation of the cysteine desulfurase activity, as a CplxIV with a catalytically dead NFS1 hardly bound iron (Table S1 in the Supporting Information).

As for frataxins from other organisms, our results show that free murine frataxin is able to bind iron, albeit to a lesser extent. However, once complexed within CplxIV, frataxin loses its ability to bind iron. The FXN iron binding site is likely not available (hidden), in agreement with mutagenesis experiments,[10,16] structural data,[10] and modeling,[28] which suggest that the surface of interaction between IscS/NFS1 and CyaY/

dx.doi.org/10.1021/ja308736e | J. Am. Chem. Soc. 2013, 135, 733–740

FXN involves direct recognition of the negatively charged region of frataxin (which is involved in iron binding) by the positively charged patch on IscS/NFS1.[28] Upon activation of the cysteine desulfurase through FXN, iron enters within CplxIV. These results demonstrate that iron loading is dependent on sulfur production, thus suggesting a concerted mechanism for iron and sulfur arrival on CplxIV rather than a sequential mechanism. This question was addressed in previous studies using either free scaffold (IscU) or carrier (SufA) proteins without conclusive answers.[33−35] Although our data cannot rule out the possibility that sulfur arrives first, they clearly demonstrate that iron cannot arrive first. The Fe−S biogenesis mechanism should be further explored using the assembly complex rather than the free individual components to resolve this key question.

Both Complexes Assemble $[Fe_4S_4]$ Clusters, Which Are More Efficiently Transferred in the Presence of Frataxin. We investigated whether the presence of excess iron and the concomitant activation of cysteine desulfurase lead to the formation of Fe−S clusters within the complexes. We first analyzed CplxIV using UV−vis absorption, electron paramagnetic resonance (EPR), and Mössbauer spectroscopy. The absolute absorption variations of CplxIV during reconstitution (using a 4-fold molar excess of Fe^{2+}) monitored by UV−vis spectroscopy (Figure 4A inset) showed an increase in the characteristic S → Fe^{3+} charge-transfer band at 420 nm simultaneously with the appearance of a dark-brown color in the solution (Figure 4A). After desalting, the reconstituted complex (CplxIV-R) contained 6 ± 0.95 S/Cplx and 3.5 ± 0.04 Fe/Cplx, values that were obtained within 15 min when the complex was incubated with Fe and cysteine (Figure S5A in the Supporting Information). This value was unchanged after analysis of the sample by size-exclusion chromatography (SEC) (Figure S6A in the Supporting Information). A representative Mössbauer spectrum of CplxIV-R is depicted in Figure 4B. As is typical for reconstituted Fe−S proteins, the spectrum comprises several components: two major lines at −0.1 and +1.3 mm/s flanked by a broad peak at 2.5 mm/s in addition to a featureless component extending from −5 to +5 mm/s (most easily seen at high Fe^{2+}). The central lines could be modeled using a quadrupole doublet whose isomer shift [δ = 0.44(3) mm/s] and quadrupole splitting [ΔE_Q = 1.09(6) mm/s] are indicative of an $[Fe_4S_4]^{2+}$ cluster. This assignment is supported by the fact that the main features of the spectrum recorded with an applied magnetic field of 7 T (Figure 4C) could be reproduced using the above parameters assuming a spin S = 0, as expected for an $[Fe_4S_4]^{2+}$ cluster.

Quantification of the main quadrupole doublet indicated that 42% of the iron belonged to the $[Fe_4S_4]^{2+}$ clusters. Similar values were found using 2−10 equiv of Fe^{2+} provided that the incubation time reached 1 h (Table S2 in the Supporting Information). The peak at 2.5 mm/s can originate from high-spin S = 2 ferrous species, with the abnormal shape and broadening of the line being due to a mixture of hexa- and tetracoordinate Fe^{II} species. Assembly of the Fe−S cluster on CplxIV did not induce any dissociation of the complex, as assessed by the SEC elution profile on Superdex-200 (Figure S6A in the Supporting Information).

Under reconstitution conditions identical to those for CplxIV, the absolute absorption variations during reconstitution of CplxIII indicated the formation of Fe−S clusters (Figure 5A inset). During this process, CplxIII-R displayed a reddish-brown color (Figure 5A). As for CplxIV-R, no dissociation of the complex occurred once an Fe−S cluster was built (Figure S6B in the Supporting Information). CplxIII-R contained a maximum of 1.8 ± 0.2 Fe/Cplx and 2 ± 0.1 S/Cplx, contents that were reached within the first 15 min of the reconstitution,

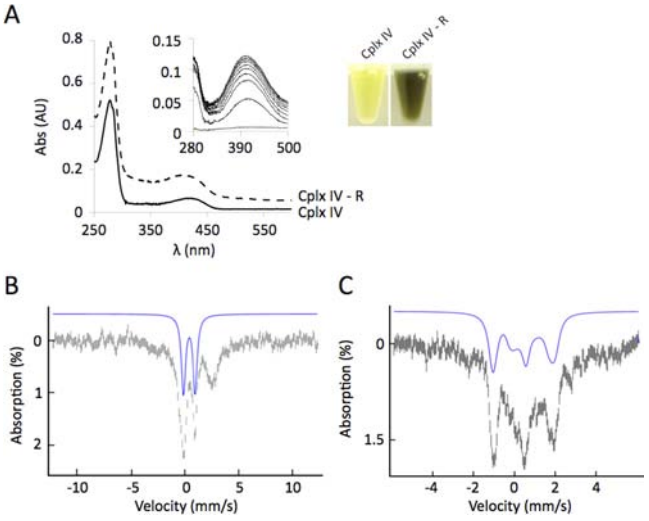

Figure 4. Fe−S cluster reconstitution on the quaternary complex. (A) UV−vis profiles of the quaternary complex before and after reconstitution. Insets: (left) absolute UV−vis absorbance variations during reconstitution (4 equiv of Fe^{2+}, 10 equiv of cysteine, and 50 equiv of DTT followed by desalting) and (right) CplxIV colors before and after reconstitution (CplxIV and CplxIV-R, respectively). (B, C) Mössbauer spectra of CplxIV-R (3.5 Fe/Cplx) taken at 4.2 K with an external magnetic field of (B) 0.06 and (C) 7 T applied parallel to the γ rays. The blue lines represent the contributions from $[Fe_4S_4]^{2+}$ clusters with parameters indicated in the text.

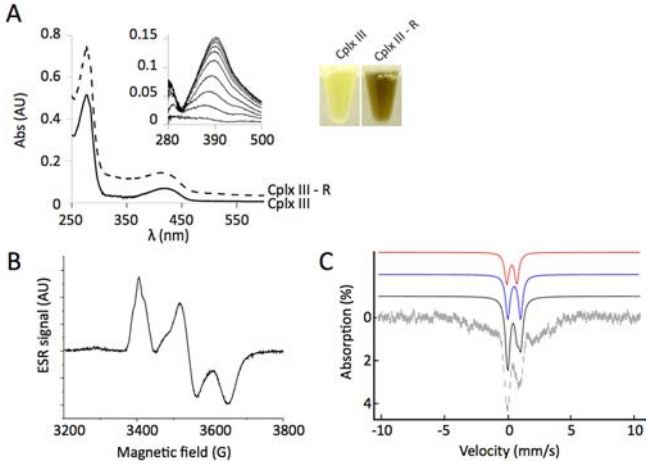

Figure 5. Fe−S cluster reconstitution on the ternary complex. (A) UV−vis profiles of the ternary complex before and after reconstitution (10 equiv of Fe^{2+}, 10 equiv of cysteine, and 50 equiv of DTT followed by desalting). Insets: (left) absolute UV−vis absorbance variations during reconstitution and (right) CplxIII color before and after reconstitution (CplxIII and CplxIII-R, respectively). (B) EPR signal of CplxIII-R (250 μM) recorded at 30 K with a microwave power of 0.5 mW. (C) Mössbauer spectrum of CplxIII-R (2.4 Fe/Cplx) taken at 4.2 K with an external magnetic field of 0.06 T applied parallel to the γ rays. The blue, red, and black solid lines represent the contributions from $[Fe_4S_4]^{2+}$ and $[Fe_2S_2]^{2+}$ clusters and their sum, respectively, with the parameters indicated in the text.

dx.doi.org/10.1021/ja308736e | J. Am. Chem. Soc. 2013, 135, 733−740

as for CplxIV-R (Figure S5A in the Supporting Information). This content could not be further increased despite the addition of a greater excess of iron to the complex and remained after SEC on Superdex-200. CplxIII-R was reproducibly EPR-active with an $S = {}^1/_2$ species characterized by a rhombic signal (g values of 2.026, 1.947, and 1.889; g_{av}= 1.954) that integrated for 16% of the total iron of the complex (Figure 5B). These g values are similar to those observed for the $[Fe_2S_2]^+$ cluster of plant ferredoxin.[36] The temperature dependence and microwave power saturation properties (signal visible up to 60 K without broadening) also pointed to an $[Fe_2S_2]^+$ cluster. CplxIV-R exhibited the same signal but with a very low intensity (Figure S5B in the Supporting Information). Figure 5C presents a representative Mössbauer spectrum of the CplxIII-R complex that was recorded as in Figure 4C for the quaternary complex. Whereas the two spectra are globally similar, significant differences exist. Indeed, the higher-velocity line of the central doublet appears abnormally broad, and this effect is maximized at high Fe^{2+} concentration. It follows that the central doublet could not be simulated with a single component. By contrast, a good simulation was obtained by considering that two species, an $[Fe_4S_4]^{2+}$ cluster and an $[Fe_2S_2]^{2+}$ cluster, contribute to this doublet. The simulation presented in Figure 5C was obtained by including a 19% contribution of an $[Fe_2S_2]^{2+}$ cluster as found in IscU (average parameters δ = 0.29 mm/s and ΔE_Q = 0.78 mm/s) in addition to 27% contribution of an $[Fe_4S_4]^{2+}$ cluster with parameters δ = 0.45(3) mm/s and ΔE_Q = 0.98(6) mm/s, similar to those of the quaternary complex. The featureless component extending from −5 to 5 mm/s may come from adventitiously bound iron species and/or reduced $[Fe_4S_4]^+$ and $[Fe_2S_2]^+$ clusters, as observed by EPR for the latter. Taken together, these results demonstrate that CplxIII-R can assemble in vitro both $[Fe_2S_2]$ clusters in the 1+ and 2+ states and $[Fe_4S_4]^{2+}$ clusters.

We finally investigated whether CplxIII-R and CplxIV-R could provide their $[Fe_4S_4]$ clusters to target enzymes by incubating them anaerobically with the apo form of mammalian mitochondrial aconitase (mACO2), a well-characterized $[Fe_4S_4]$ protein.[37] mACO2 was pretreated with dithiothreitol (DTT), desalted, and then incubated with either 2.5 equiv of CplxIII-R or 1.25 equiv of CplxIV-R in order to provide the same amounts of $[Fe_4S_4]$ cluster to mACO2. Under such conditions, the control containing apo-mACO2 and an excess of Fe^{2+} and S^{2-} gave an activity of 15.0 ± 1.9 nmol min^{-1} mg^{-1}. CplxIII-R could also mature aconitase (18.2 ± 1.4 nmol min^{-1} mg^{-1}) to a level similar to that obtained using free iron and sulfide. By contrast, CplxIV-R activated mACO2 with an enzymatic activity of 46.2 ± 2.1 nmol of NADPH min^{-1} mg^{-1}, which is 3-fold higher than those of the control and CplxIII-R (Figure 6). This demonstrates that CplxIV-R is more efficient in maturing mACO2 than either CplxIII-R or free iron and sulfide.

Addition of increasing concentrations of a strong Fe chelator, bathophenanthroline, to the standard reaction mixture had little effect on the Fe−S cluster transfer from CplxIV-R to mACO2 (17% loss at 30 μM). At the same concentration, bathophenanthroline inhibited roughly completely the cluster transfer from CplxIII-R (83% loss) (Figure 6). Interestingly, cluster transfer from CplxIII-R closely parallels that of chemical reconstitution. This suggests that cluster transfer to mACO2 from CplxIII-R is likely due in part to release of Fe−S in the medium, while cluster transfer from CplxIV-R is a concerted process.

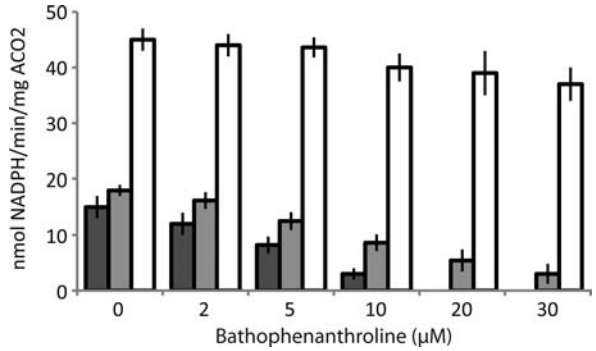

Figure 6. Fe−S cluster transfer from CplxIII-R and CplxIV-R to apo-mACO2. Aconitase activity was measured after transfer of the $[Fe_4S_4]$ cluster from CplxIII-R (gray bars) or CplxIV-R (white bars) in the presence of increasing amounts of the iron chelator bathophenanthroline. The mACO2 activity control was measured upon addition of a 4-fold molar excess of Fe^{2+} and S^{2-} (black bars). The mACO2 activity was measured after 30 min of incubation with 2.5 equiv of CplxIII-R (2 Fe/Cplx) or 1.25 equiv of CplxIV-R (4 Fe/Cplx), respectively. All of the experiments were done under anaerobic conditions at 17 °C.

Taken together, these results demonstrate that CplxIII-R and CplxIV-R assemble mainly $[Fe_4S_4]^{2+}$ clusters in vitro. This is the first time that an Fe−S cluster has been observed and characterized spectroscopically on mammalian ISC assembly complexes. There are 2 ISCU/Cplx, and our quantification demonstrates that there is reproducibly no more than 0.4 and 0.27 $[Fe_4S_4]$ cluster per CplxIV-R and CplxIII-R, respectively. As there is no dissociation of CplxIV-R after Fe−S assembly, our results suggest that only one ISCU of CplxIV-R is metalated. It is tempting to propose that only one unit of CplxIV-R is active, maybe by negative-cooperative regulation between the subunits through structural changes, as has been proposed for other PLP enzymes.[38] Interestingly, the same amount of high-spin ferrous iron on CplxIV-R was also consistently found. Whether this iron is located on the second ISCU of CplxIV-R and its physiological relevance are currently under investigation. Furthermore, for the first time, an $[Fe_2S_2]^+$ species was also observed on the mammalian Fe−S assembly machinery. This is surprising considering that no reducing agent typically used to observe such a species (e.g., dithionite) was present in the reaction. DTT was probably responsible for the formation of this species, as observed on the bacterial Fe−S carrier SufA.[39] The fact that it is observable mainly on CplxIII-R likely results because CplxIII-R contains a greater amount of $[Fe_4S_4]^{2+}$ clusters with regard to total iron. The $[Fe_2S_2]^+$ species may correspond to an intermediate in the formation of $[Fe_4S_4]^{2+}$ clusters from $[Fe_2S_2]^{2+}$ clusters, as proposed for the general $[Fe_4S_4]$ assembly process[40] and recently demonstrated in the case of ^{nif}IscA.[41] In this respect, it is worth noting that the successive formation of $[Fe_2S_2]^{2+}$ and $[Fe_4S_4]^{2+}$ clusters has been observed in the bacterial system.[42] In agreement with an enhancement of the cysteine desulfurase activity in the presence of frataxin, neither $[Fe_2S_2]^{2+}$ species nor $[Fe_2S_2]^+$ intermediates were observed on CplxIV-R (Table S2 in the Supporting Information). Finally, in contrast to CplxIII-R, CplxIV-R is able to mature mACO2. However, the mACO2 activity obtained with CplxIV-R is low compared with that of a reconstituted mACO2 (200 nmol of NADPH min^{-1} mg^{-1}), suggesting that some components needed for total and efficient Fe−S transfer are missing, such as the chaperones and/or ferredoxin.

CONCLUSION

To the best of our knowledge, this is the first demonstration that both CplxIII and CplxIV of the mammalian Fe−S assembly machinery can assemble $[Fe_4S_4]$ clusters without dissociation of the complexes. Our results also provide evidence that mammalian frataxin stabilizes CplxIII and controls iron entry on CplxIV through activation of its cysteine desulfurase activity. The presence of FXN leads to a greater amount of $[Fe_4S_4]$ cluster per complex and to a transferable $[Fe_4S_4]$ cluster. The properties of CplxIII-R are consistent with the biochemical phenotype associated with Friedreich's ataxia and with Friedreich's ataxia conditional mouse models that show residual Fe−S enzyme activities in the absence of frataxin.[43,44] Our results provide consolidated information that is crucial for unraveling both the Fe−S cluster assembly process and the molecular basis of Friedreich's ataxia. Further work using these complexes with the addition of other essential components of the Fe−S assembly and transfer machinery should be performed to understand this essential metabolic pathway.

EXPERIMENTAL SECTION

Recombinant CplxIV was obtained by coexpression of murine NFS1, ISD11, ISCU, and FXN-His in *E. coli* and purified as reported previously,[16] except that an affinity cobalt column was used. Recombinant CplxIII was obtained by coexpression of murine NFS1, ISD11, and ISCU-His in *E. coli* and purified as for CplxIV. GST-mACO2 production and purification were carried out as previously described.[16] The quaternized complex was obtained by mixing CplxIII with a 3-fold excess of free FXN. Protein-bound iron and sulfur quantitations were carried out as previously described.[45,46] AUC sedimentation experiments were used to determine the affinity of FXN to CplxIII. The cysteine desulfurase activity of complexes was determined as detailed for alanine production[47] and for sulfide release.[45] Fe−S cluster assembly on CplxIII and CplxIV was performed using L-cysteine and a ferrous iron salt as the sulfur and iron sources, respectively, as reported previously,[48] and the Fe−S transfer experiment to aconitase was performed as detailed elsewhere.[49] Structural characterization of CplxIII and CplxIV was performed by UV−vis absorption, Mössbauer, and EPR spectroscopy.

ASSOCIATED CONTENT

Supporting Information

Experimental methods for expressing, purifying, and assaying the proteins used in this work; protocols used for cluster transfer reactions; and spectroscopic analyses for Fe−S cluster characterization. This material is available free of charge via the Internet at http://pubs.acs.org.

AUTHOR INFORMATION

Corresponding Author

hpuccio@igbmc.fr; sollagnier@cea.fr

Notes

The authors declare no competing financial interest.

ACKNOWLEDGMENTS

We thank N. Levy, F. Klein, and A. Hick (IGBMC, Strasbourg) for technical help and S. Schmucker (IGBMC, Strasbourg), E. Mulliez (CBM, Grenoble), and M. Fontecave (Collège de France, Paris) for scientific discussions and suggestions. This work was supported by the European Community under the European Research Council [206634/ISCATAXIA] (to H.P.) and the Seventh Framework Programme [242193/EFACTS] (to H.P.). F.C. was a recipient of a Ph.D. fellowship from La Fondation Sébastien Grosjean contre les Maladies Orphelines. J.-M.L. acknowledges the support of the Région Rhone-Alpes through Contract CIBLE 07 016335, and S.O.d.C. acknowledges the support of the ANR FeStreS.

REFERENCES

(1) Lill, R. *Nature* **2009**, *460*, 831.
(2) Fontecave, M.; Ollagnier-de-Choudens, S. *Arch. Biochem. Biophys.* **2008**, *474*, 226.
(3) Johnson, D. C.; Dean, D. R.; Smith, A. D.; Johnson, M. K. *Annu. Rev. Biochem.* **2005**, *74*, 247.
(4) Rouault, T. A. *Dis. Models Mech.* **2012**, *5*, 155.
(5) Wiedemann, N.; Urzica, E.; Guiard, B.; Müller, H.; Lohaus, C.; Meyer, H. E.; Ryan, M. T.; Meisinger, C.; Mühlenhoff, U.; Lill, R.; Pfanner, N. *EMBO J.* **2006**, *25*, 184.
(6) Pandey, A.; Yoon, H.; Lyver, E. R.; Dancis, A.; Pain, D. *J. Biol. Chem.* **2011**, *286*, 38242.
(7) Adam, A. C.; Börnhovd, C.; Prokisch, H.; Neupert, W.; Hell, K. *EMBO J.* **2006**, *25*, 174.
(8) Raulfs, E. C.; O'Carroll, I. P.; Dos Santos, P. C.; Unciuleac, M. C.; Dean, D. R. *Proc. Natl. Acad. Sci. U.S.A.* **2008**, *105*, 8591.
(9) Marinoni, E. N.; de Oliveira, J. S.; Nicolet, Y.; Raulfs, E. C.; Amara, P.; Dean, D. R.; Fontecilla-Camps, J. C. *Angew. Chem., Int. Ed.* **2012**, *51*, 5439.
(10) Shi, R.; Proteau, A.; Villarroya, M.; Moukadiri, I.; Zhang, L.; Trempe, J. F.; Matte, A.; Armengod, M. E.; Cygler, M. *PLoS Biol.* **2010**, *8*, No. e1000354.
(11) Layer, G.; Ollagnier-de Choudens, S.; Sanakis, Y.; Fontecave, M. *J. Biol. Chem.* **2006**, *281*, 16256.
(12) Chandramouli, K.; Unciuleac, M. C.; Naik, S.; Dean, D. R.; Huynh, B. H.; Johnson, M. K. *Biochemistry* **2007**, *46*, 6804.
(13) Campuzano, V.; Montermini, L.; Molto, M. D.; Pianese, L.; Cossee, M.; Cavalcanti, F.; Monros, E.; Rodius, F.; Duclos, F.; Monticelli, A.; Zara, F.; Canizares, J.; Koutnikova, H.; Bidichandani, S. I.; Gellera, C.; Brice, A.; Trouillas, P.; De Michele, G.; Filla, A.; De Frutos, R.; Palau, F.; Patel, P. I.; Di Donato, S.; Mandel, J. L.; Cocozza, S.; Koenig, M.; Pandolfo, M. *Science* **1996**, *271*, 1423.
(14) Schmucker, S.; Puccio, H. *Hum. Mol. Genet.* **2010**, *19*, R103.
(15) Tsai, C. L.; Barondeau, D. P. *Biochemistry* **2010**, *49*, 9132.
(16) Schmucker, S.; Martelli, A.; Colin, F.; Page, A.; Wattenhofer-Donze, M.; Reutenauer, L.; Puccio, H. *PLoS One* **2011**, *6*, No. e16199.
(17) Adinolfi, S.; Iannuzzi, C.; Prischi, F.; Pastore, C.; Iametti, S.; Martin, S. R.; Bonomi, F.; Pastore, A. *Nat. Struct. Mol. Biol.* **2009**, *16*, 390.
(18) Huynen, M. A.; Snel, B.; Bork, P.; Gibson, T. J. *Hum. Mol. Genet.* **2001**, *10*, 2463.
(19) Mühlenhoff, U.; Richhardt, N.; Ristow, M.; Kispal, G.; Lill, R. *Hum. Mol. Genet.* **2002**, *11*, 2025.
(20) Yoon, T.; Cowan, J. A. *J. Am. Chem. Soc.* **2003**, *125*, 6078.
(21) Nair, M.; Adinolfi, S.; Pastore, C.; Kelly, G.; Temussi, P.; Pastore, A. *Structure* **2004**, *12*, 2037.
(22) Cook, J. D.; Bencze, K. Z.; Jankovic, A. D.; Crater, A. K.; Busch, C. N.; Bradley, P. B.; Stemmler, A. J.; Spaller, M. R.; Stemmler, T. L. *Biochemistry* **2006**, *45*, 7767.
(23) Gerber, J.; Mühlenhoff, U.; Lill, R. *EMBO Rep.* **2003**, *4*, 906.
(24) Gakh, O.; Park, S.; Liu, G.; Macomber, L.; Imlay, J. A.; Ferreira, G. C.; Isaya, G. *Hum. Mol. Genet.* **2006**, *15*, 467.
(25) Adamec, J.; Rusnak, F.; Owen, W. G.; Naylor, S.; Benson, L. M.; Gacy, A. M.; Isaya, G. *Am. J. Hum. Genet.* **2000**, *67*, 549.
(26) Aloria, K.; Schilke, B.; Andrew, A.; Craig, E. A. *EMBO Rep.* **2004**, *5*, 1096.
(27) Gakh, O.; Bedekovics, T.; Duncan, S. F.; Smith, D. Y., IV; Berkholz, D. S.; Isaya, G. *J. Biol. Chem.* **2010**, *285*, 38486.
(28) Prischi, F.; Konarev, P. V.; Iannuzzi, C.; Pastore, C.; Adinolfi, S.; Martin, S. R.; Svergun, D. I.; Pastore, A. *Nat. Commun.* **2010**, *1*, 95.
(29) Furne, J.; Saeed, A.; Levitt, M. D. *Am. J. Physiol.: Regul., Integr. Comp. Physiol.* **2008**, *295*, R1479.
(30) Kato, S.; Mihara, H.; Kurihara, T.; Takahashi, Y.; Tokumoto, U.; Yoshimura, T.; Esaki, N. *Proc. Natl. Acad. Sci. U.S.A.* **2002**, *99*, 5948.

(31) Loiseau, L.; Ollagnier-de-Choudens, S.; Nachin, L.; Fontecave, M.; Barras, F. *J. Biol. Chem.* **2003**, *278*, 38352.
(32) Bridwell-Rabb, J.; Iannuzzi, C.; Pastore, A.; Barondeau, D. P. *Biochemistry* **2012**, *51*, 2506.
(33) Sendra, M.; Ollagnier de Choudens, S.; Lascoux, D.; Sanakis, Y.; Fontecave, M. *FEBS Lett.* **2007**, *581*, 1362.
(34) Nuth, M.; Yoon, T.; Cowan, J. A. *J. Am. Chem. Soc.* **2002**, *124*, 8774.
(35) Smith, A. D.; Agar, J. N.; Johnson, K. A.; Frazzon, J.; Amster, I. J.; Dean, D. R.; Johnson, M. K. *J. Am. Chem. Soc.* **2001**, *123*, 11103.
(36) Gambarelli, S.; Mouesca, J. M. *Inorg. Chem.* **2004**, *43*, 1441.
(37) Dupuy, J.; Volbeda, A.; Carpentier, P.; Darnault, C.; Moulis, J. M.; Fontecilla-Camps, J. C. *Structure* **2006**, *14*, 129.
(38) Selbach, B.; Earles, E.; Dos Santos, P. C. *Biochemistry* **2010**, *49*, 8794.
(39) Gupta, V.; Sendra, M.; Naik, S. G.; Chahal, H. K.; Huynh, B. H.; Outten, F. W.; Fontecave, M.; Ollagnier de Choudens, S. *J. Am. Chem. Soc.* **2009**, *131*, 6149.
(40) Krebs, C.; Agar, J. N.; Smith, A. D.; Frazzon, J.; Dean, D. R.; Huynh, B. H.; Johnson, M. K. *Biochemistry* **2001**, *40*, 14069.
(41) Mapolelo, D. T.; Zhang, B.; Naik, S. G.; Huynh, B. H.; Johnson, M. K. *Biochemistry* **2012**, *51*, 8071.
(42) Agar, J. N.; Krebs, C.; Frazzon, J.; Huynh, B. H.; Dean, D. R.; Johnson, M. K. *Biochemistry* **2000**, *39*, 7856.
(43) Puccio, H.; Simon, D.; Cossee, M.; Criqui-Filipe, P.; Tiziano, F.; Melki, J.; Hindelang, C.; Matyas, R.; Rustin, P.; Koenig, M. *Nat. Genet.* **2001**, *27*, 181.
(44) Martelli, A.; Wattenhofer-Donze, M.; Schmucker, S.; Bouvet, S.; Reutenauer, L.; Puccio, H. *Hum. Mol. Genet.* **2007**, *16*, 2651.
(45) Beinert, H. *Anal. Biochem.* **1983**, *131*, 373.
(46) Fish, W. W. *Methods Enzymol.* **1988**, *158*, 357.
(47) Yoshida, A. *Anal. Biochem.* **1965**, *11*, 383.
(48) Wollers, S.; Layer, G.; Garcia-Serres, R.; Signor, L.; Clemancey, M.; Latour, J. M.; Fontecave, M.; Ollagnier de Choudens, S. *J. Biol. Chem.* **2010**, *285*, 23331.
(49) Tsaousis, A. D.; Ollagnier de Choudens, S.; Gentekaki, E.; Long, S.; Gaston, D.; Stechmann, A.; Vinella, D.; Py, B.; Fontecave, M.; Barras, F.; Lukes, J.; Roger, A. J. *Proc. Natl. Acad. Sci. U.S.A.* **2012**, *109*, 10426.